Temperature-disorder phase diagram of a three-dimensional gauge-glass model

Vincenzo Alba*
Max-Planck-Institut für Physik komplexer Systeme, D-01187 Dresden, Germany
Scuola Normale Superiore and INFN, I-56126 Pisa, Italy

Ettore Vicari†
Dipartimento di Fisica dell'Università di Pisa and INFN, I-56127 Pisa, Italy

(Received 15 December 2010; revised manuscript received 9 February 2011; published 25 March 2011)

We investigate the temperature-disorder (T-σ) phase diagram of a three-dimensional gauge glass model, which is a cubic-lattice nearest-neighbor XY model with quenched random phase shifts A_{xy} at the bonds. We consider the uncorrelated phase-shift distribution $P(A_{xy}) \sim \exp[(\cos A_{xy})/\sigma]$, which has the pure XY model, and the uniform distribution of random phase shifts as extreme cases at $\sigma = 0$ and $\sigma \to \infty$, respectively, and which gives rise to equal magnetic and overlap correlation functions when $T = \sigma$. Our study is mostly based on numerical Monte Carlo simulations. While the high-temperature phase is always paramagnetic, at low temperatures there is a ferromagnetic phase for weak disorder (small σ) and a glassy phase at large disorder (large σ). These three phases are separated by transition lines with different magnetic and glassy critical behaviors. The disorder induced by the random phase shifts turns out to be irrelevant at the paramagnetic-ferromagnetic transition line, where the critical behavior belongs to the 3D XY universality class of pure systems; disorder gives rise only to very slowly decaying scaling corrections. The glassy critical behavior along the paramagnetic-glassy transition line belongs to the gauge-glass universality class, with a quite large exponent $\nu = 3.2(4)$. These transition lines meet at a multicritical point M, located at $T_M = \sigma_M = 0.7840(2)$. The low-temperature ferromagnetic and glassy phases are separated by a third transition line, from M down to the $T = 0$ axis, which is slightly reentrant.

DOI: 10.1103/PhysRevB.83.094203 PACS number(s): 64.60.F−, 75.50.Lk, 05.70.Fh, 74.62.En

I. INTRODUCTION AND SUMMARY

Spin glass models are simplified, although still quite complex, models retaining the main features of physical systems which show glassy phases. They may be considered theoretical laboratories where the combined effects of quenched disorder and frustration can be studied. Their phase diagrams and critical behaviors provide examples of possible scenarios which can be used to interpret the experimental results of complex materials. For example, Ising-type spin glasses, such as the $\pm J$ Ising model,[1] model disordered uniaxial magnetic materials characterized by random ferromagnetic and antiferromagnetic short-range interactions. While many theoretical and numerical works have been devoted to the study of the phase diagrams and the magnetic and glassy critical behaviors of Ising-like spin glasses, see, e.g., Refs. 2–4 and references therein, much less is known about the thermodynamic properties of spin glass models with continuous symmetries. In the case of the Heisenberg spin glass there is some evidence for a glassy transition at finite temperature T, but its nature is still debated, see, e.g., Refs. 5,6 and references therein.

Another physically interesting spin glass model is the XY model with random phase shifts, also known as the gauge-glass model, which is characterized by a global U(1) symmetry. It has been proposed as a simplified model of disordered granular superconductors to describe vortex-glass transitions.[7–13] The phase diagram and critical behaviors of two-dimensional (2D) gauge glasses have been much investigated, see, e.g., Refs. 14,15 and references therein. It is now well established that at weak disorder there is a low-T quasi-long-range order phase separated by a Kosterlitz-Thouless transition line from the paramagnetic phase; no glassy phase exists at finite T, but a $T = 0$ glassy critical behavior at sufficiently large disorder. A discussion of the general temperature-disorder phase diagram of the three-dimensional (3D) gauge glass can be found in Refs. 16,17. The ferromagnetic phase of the pure cubic-lattice XY model is expected to survive at weak disorder,[18] while it should disappear at large disorder, where a low-T glassy phase may exist. Several numerical works have addressed the existence of a vortex-glass phase at finite T in the case of a uniform random-shift distribution,[19–31] providing evidence of a finite-T glassy transition. Apart from these results for the extreme disordered case, the phase diagram and the critical behaviors at the different transition lines have not been numerically investigated yet. We also mention that experimental results for vortex glass phases in superconductors have been reported in Refs. 32–36, but the experimental scenario for the behavior at the transition does not appear settled yet.

In this paper we investigate the temperature-disorder phase diagram of the 3D gauge glass and its critical behaviors along the transition lines which separate the different phases.

The 3D gauge-glass model is defined by the partition function

$$Z(\{A\}) = \int [D\psi] \exp(-\mathcal{H}/T),$$
$$\mathcal{H} = -\sum_{\langle xy \rangle} \mathrm{Re}\, \bar{\psi}_x U_{xy} \psi_y = -\sum_{\langle xy \rangle} \cos(\theta_x - \theta_y - A_{xy}), \quad (1)$$

where $\psi_x \equiv e^{i\theta_x}$, $U_{xy} \equiv e^{iA_{xy}}$, and the sum runs over the bonds $\langle xy \rangle$ of a cubic lattice. The phases A_{xy} are uncorrelated quenched random variables with zero average. A Gaussian distribution $P_G(A_{xy}) \propto \exp[-A_{xy}^2/(2\sigma)]$ is often considered in the studies of gauge glasses. In this paper we consider a

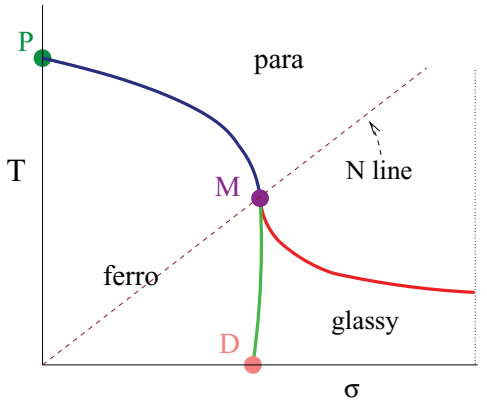

FIG. 1. (Color online) Sketch of the temperature-disorder (T-σ) phase diagram of the 3D gauge glass.

slightly different *cosine* distribution

$$P(A_{xy}) \propto \exp\left(\frac{\cos A_{xy}}{\sigma}\right). \qquad (2)$$

Analogously to the Gaussian distribution, we recover the pure cubic-lattice XY model for $\sigma \to 0$ and uniformly distributed random phase shifts in the limit $\sigma \to \infty$. The cosine distribution is particularly interesting because it lends itself to some exact relations along the so-called Nishimori (N) line $T = \sigma$[16,17], such as the equality of the magnetic and overlap correlation functions, which are useful to identify the multicritical point where the transition lines meet in the T-σ phase diagram.

Our study of the T-σ phase diagram, and the magnetic and glassy critical behaviors along its transition lines, is mostly based on numerical Monte Carlo (MC) simulations. Supplementing the numerical results with renormalization-group (RG) and finite-size scaling (FSS) analyses, we arrive at the phase diagram sketched in Fig. 1. In Fig. 2 we show where we performed the MC simulations in the T-σ plane. Our main results are the following.

While the high-T phase is always paramagnetic, at low T we have a ferromagnetic phase for weak disorder (small σ) and a glassy phase at sufficiently large disorder (large σ). These three phases are separated by different transition lines: a paramagnetic-ferromagnetic (PF) transition line, a paramagnetic-glassy (PG) transition line, and a ferromagnetic-glassy (FG) transition line, meeting at a multicritical point M located along the N line. The phase diagram of 3D gauge glasses presents several analogies with the temperature-disorder phase diagram of 3D $\pm J$ Ising spin glasses,[3,4] where analogous phases and transition lines appear.

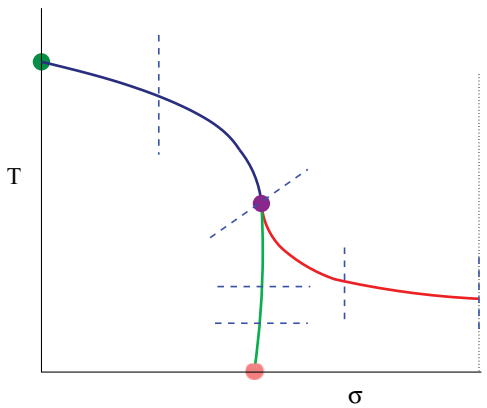

FIG. 2. (Color online) The dashed lines sketch the T and σ values of our MC simulations.

The 3D gauge glass shows different magnetic and glassy critical behaviors at the transition lines separating the different phases.

We argue that the disorder induced by the random phase shifts is irrelevant at the PF transition line starting from the pure XY transition point for $\sigma = 0$, at[37] $T_{XY} = 2.201\,842(5)$. Thus the asymptotic critical behavior belongs to the 3D XY universality class of pure systems with U(1) symmetry, characterized by the correlation-length critical exponent[37] $\nu_{XY} = 0.6717(1)$. Analogously to randomly dilute 3D XY models,[38] the disorder induces new scaling corrections which get suppressed very slowly, as $O(\xi^{-\omega_d})$ where ξ is the critical length scale and $\omega_d = 3 - 2/\nu_{XY} = 0.0225(5)$. A FSS analysis of MC simulations at $\sigma = 0.35$, up to $L = 30$, supports this critical behavior. The PF transition line ends at the multicritical point M located at $T_M = \sigma_M \approx 0.784$ along the N line. For comparison, we mention that, unlike the gauge-glass model, the quenched disorder is relevant at the PF transition line of the 3D $\pm J$ Ising models, giving rise to a new universality class, which is the same universality class of the 3D randomly dilute Ising systems.[38,39]

A low-T glassy phase appears for sufficiently large disorder, i.e., $\sigma \gtrsim \sigma_M$, separated by a finite-T PG transition line from the paramagnetic phase. A reasonable hypothesis is that the glassy critical behavior is universal along the PG transition line, up to $\sigma \to \infty$ (i.e., the model with uniform disorder distribution), and belongs to the 3D gauge-glass universality class. This is supported by MC simulations for $\sigma = 4/3$ and for the uniform random-shift distribution, up to lattice size $L = 20$, which provides clear evidence of finite-T transitions in both cases, and of the universality of their glassy critical behaviors. Moreover, their FSS analyses give $T_c = 0.475(10)$ and $T_c = 0.46(1)$ respectively for $\sigma = 4/3$ and $\sigma \to \infty$, and the estimates $\nu = 3.2(4)$ and $\eta = -0.47(2)$ for the universal exponents describing the critical overlap correlations. These critical exponents may be compared with those of the glassy transition in Ising-like spin glasses, where[4,40–42] $\nu = 2.45(15)$ and $\eta = -0.375(10)$.

The PF and PG transition lines meet at the critical point M along the N line, see Fig. 1. Actually, M is a multicritical point, characterized by a magnetic-glassy multicritical behavior with two relevant perturbations (in the absence of external fields). The tangents at M of the transition lines are parallel to the T axis. Indeed, as proved in Ref. 16, σ_M is an upper bound for the values of σ where the ferromagnetic phase can exist. A FSS analysis of MC simulations along the N line, up to $L = 20$, locates the point M at $T_M = \sigma_M = 0.7840(2)$ and provides the estimates $y_1 = 0.93(3)$ and $y_2 = 0.56(3)$ for the RG dimensions of the relevant perturbations, thus a crossover exponent $\phi \equiv y_1/y_2 = 1.7(1)$. Moreover, the exponent η associated with the spin and overlap correlation functions is $\eta = -0.121(1)$. Again, these critical exponents may be compared with those at the multicritical point of the phase

diagram of the 3D $\pm J$ Ising model where the PF and PG transition lines meet, which are[43] $y_1 = 1.02(5)$, $y_2 = 0.61(2)$, $\phi = 1.67(10)$, and $\eta = -0.114(3)$.

A transition line separating the low-T ferromagnetic and glassy phases starts from the multicritical point M toward the $T = 0$ axis, see Fig. 1. The order parameter is provided by the magnetic variables and their correlations, which become effectively paramagnetic in the glassy phase. We present FSS analyses of MC simulations at fixed $T < T_M$ up to $L = 12$. They show that the FG transition line runs almost parallel to the T axis. It is slightly reentrant; indeed, we find $\sigma_c = 0.777(2)$ at $T = 0.376$. The magnetic critical behavior varying T is compatible with a universal critical behavior along the FG transition line, with critical exponent $\nu = 1.0(1)$.

The main features of the phase diagram and the universality classes of the magnetic and glassy critical behaviors at the different transition lines are expected to be largely independent of the detail of the distribution. For example, they are expected to apply to the case of random phase shifts with Gaussian distribution.

The paper is organized as follows. Section II provides the definitions of the quantities considered in our work. In Sec. III we discuss the phase diagram at low disorder and the critical behavior at the PF transition line. In Sec. IV we focus on the the phase diagram at large disorder, i.e., large values of σ, where the low-T phase is glassy, and study the glassy critical behavior at the PG transition line. In Sec. V we study the multicritical behavior at the point M of the phase diagram, where the different transition lines meet. Finally, in Sec. VI we investigate the FG transition line, which runs from M down to the $T = 0$ axis.

II. NOTATIONS

We consider the gauge-glass model (1) defined on cubic lattices of size L^3 with periodic boundary conditions. We define the magnetic correlation function

$$G(x - y) \equiv [\langle \bar{\psi}_x \, \psi_y \rangle] \tag{3}$$

and the overlap correlation function

$$G_o(x - y) \equiv [\langle \bar{q}_x \, q_y \rangle] \equiv [\, |\langle \bar{\psi}_x \, \psi_y \rangle|^2 \,], \tag{4}$$

where q_x is the overlap variable defined as

$$q_x = \bar{\psi}_x^{(1)} \psi_x^{(2)} \tag{5}$$

using two copies $\psi_x^{(1)}$ and $\psi_x^{(2)}$ for the same disorder configuration. The angular and square brackets indicate the thermal average and the quenched average over disorder, respectively. We define the magnetic and overlap susceptibilities as

$$\chi \equiv \sum_x G(x), \quad \chi_o \equiv \sum_x G_o(x), \tag{6}$$

and the magnetic and overlap second-moment correlation lengths

$$\xi^2 \equiv \frac{\widetilde{G}(0) - \widetilde{G}(q_{\min})}{\hat{q}^2_{\min} \widetilde{G}(q_{\min})}, \quad \xi_o^2 \equiv \frac{\widetilde{G}_o(0) - \widetilde{G}_o(q_{\min})}{\hat{q}^2_{\min} \widetilde{G}_o(q_{\min})}, \tag{7}$$

where $q_{\min} \equiv (2\pi/L, 0, 0)$, $\hat{q} \equiv 2 \sin q/2$.

We also consider quantities that are invariant under RG transformations in the critical limit, such as the ratios

$$R_\xi \equiv \xi/L, \quad R_\xi^o \equiv \xi_o/L, \tag{8}$$

and the cumulants

$$U_4 \equiv \frac{[\langle |\mu|^4 \rangle]}{[\langle |\mu|^2 \rangle]^2}, \quad U_{22} \equiv \frac{[\langle |\mu|^2 \rangle^2] - [\langle |\mu|^2 \rangle]^2}{[\langle |\mu|^2 \rangle]^2}, \tag{9}$$

and

$$U_4^o \equiv \frac{[\langle |\mu_o|^4 \rangle]}{[\langle |\mu_o|^2 \rangle]^2}, \quad U_{22}^o \equiv \frac{[\langle |\mu_o|^2 \rangle^2] - [\langle |\mu_o|^2 \rangle]^2}{[\langle |\mu_o|^2 \rangle]^2}, \tag{10}$$

where $\mu \equiv \sum_x \psi_x$ and $\mu_o \equiv \sum_x q_x$. Finally, given two replicas of the system with spins $\psi_x^{(1)}$ and $\psi_x^{(2)}$, we consider the quantity[28]

$$I_o = \beta \sqrt{[\langle I^{(1)} \rangle \langle I^{(2)} \rangle]}, \tag{11}$$

where $\beta \equiv 1/T$, and

$$I^{(i)} \equiv \frac{1}{L} \sum_x \mathrm{Im}\, \bar{\psi}_x^{(i)} U_{x\, x+\hat{e}_1} \psi_{x+\hat{e}_1}^{(i)} \tag{12}$$

is the derivative of the free energy with respect to a twist along one direction $\hat{e}_1$ of the lattice.

III. THE PARAMAGNETIC-FERROMAGNETIC TRANSITION LINE

The random phase shifts of the gauge glass model (1) vanish when $\sigma \to 0$, thus recovering the pure cubic-lattice nearest-neighbor XY model, which undergoes a continuous transition at[37] $T_{XY} = 2.201\,842(5)$ between the high-T paramagnetic phase and a low-T ferromagnetic phase with long-range order. The critical behavior belongs to the 3D XY universality class,[38] characterized by the symmetry U(1), which also describes transitions related to the formation of Bose-Einstein condensates in interacting quantum particle systems, the superfluid transition in ^{4}He, transitions in easy-plane magnets, etc. The critical exponents, which determine the asymptotic behaviors of the critical correlations, are[37,38] $\nu_{XY} = 0.6717(1)$, $\eta_{XY} = 0.0381(1)$, $\alpha_{XY} = 2 - 3\nu_{XY} = -0.0151(3)$, etc.

The low-T ferromagnetic phase is expected to be stable with respect to the presence of a weak disorder respecting the global U(1) symmetry, such as that arising in the gauge glass model for nonzero values of σ (see also Ref. 18), analogously to the 2D gauge glasses[44] (where actually we have a low-T quasi-long-range order phase), and the 3D $\pm J$ Ising model,[39] where the disorder does not break the global Z_2 symmetry. Therefore we expect that a paramagnetic-ferromagnetic (PF) transition line starts from the pure XY critical point $P \equiv (\sigma = 0, T = T_{XY})$, where the relevant symmetry is still U(1).

A. Irrelevance of the disorder at the PF transition

The critical behavior along the PF line can be inferred by studying the relevance of the RG perturbation induced by the random phase shifts at the pure 3D XY fixed point. Since the random phase shifts preserve the global U(1) symmetry, we argue that the leading disorder RG perturbation gets effectively coupled to the energy density at the PF transition line, as in the case of randomly dilute spin models.[38,45] This implies

that the relevance of the disorder is related to the sign of the specific-heat exponent of the pure system.[45,46] If it is positive, like the case of 3D Ising-like models, the disorder provides a relevant perturbation, which changes the asymptotic critical behavior, giving rise to a new universality class.[39] On the other hand, if the specific-heat exponent is negative, as in the case of the 3D XY models where $\alpha_{XY} = -0.0151(3)$ [but also for any 3D model with symmetry O(N) and $N \geqslant 2$[38]], the disorder is irrelevant in the RG sense, which implies that the critical behavior belongs to the same universality class of the pure system, and the asymptotic power-law behaviors remain unchanged.

However, disorder gives rise to scaling corrections which get suppressed very slowly and are absent in the pure system. Analogously to randomly dilute 3D XY models,[38] they are $O(\xi^{-\omega_d})$ where ξ is the critical length scale and

$$\omega_d = -\frac{\alpha_{XY}}{\nu_{XY}} = 3 - \frac{2}{\nu_{XY}} = 0.0225(5), \qquad (13)$$

to be compared with the leading scaling correction of pure XY systems which are $O(\xi^{-\omega})$ with[37,38] $\omega = 0.785(20)$.

B. Monte Carlo simulations at $\sigma = 0.35$

We support the above scenario by a FSS analysis of MC simulations at $\sigma = 0.35$, up to lattice size $L = 30$. In the simulations we use both Metropolis and overrelaxed microcanonical local updatings. One single step of the Monte Carlo update is composed by one Metropolis sweep followed by five overrelaxed microcanonical sweeps. See Ref. 14 for more details. We average over a large number of samples, from $N_s = 16000$ for $L = 6$ decreasing to $N_s = 3000$ for $L = 30$. The equilibration is carefully checked by monitoring the MC time evolution of the observables which we consider.

The FSS of the RG invariant quantities, such as R_ξ, U_4, R_ξ^o, and U_4^o, show clear evidence of a continuous transition, see, e.g., Fig. 3. A standard FSS analysis gives $T_c = 1.7103(3)$ from the crossing point of their data for different values of L, and $\nu = 0.68(1)$ from their slope at T_c (using data for $L \geqslant L_{\min} \gtrsim 12$). This estimate of ν is in good agreement with the exponent $\nu_{XY} = 0.6717(1)$ of the 3D XY universality class. Indeed, Fig. 4 shows that a good collapse of the MC data of

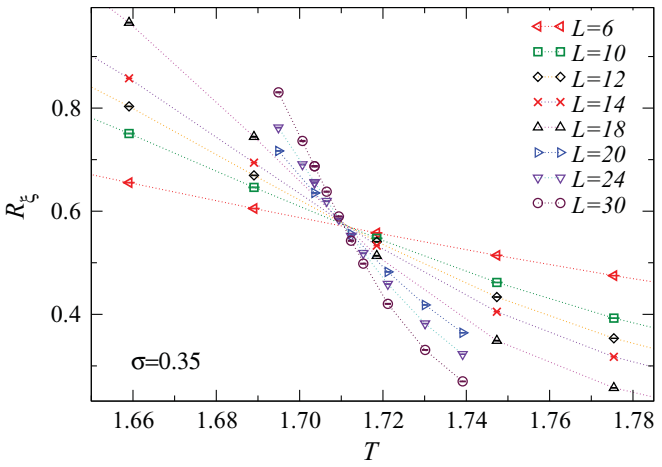

FIG. 3. (Color online) MC data of R_ξ at $\sigma = 0.35$.

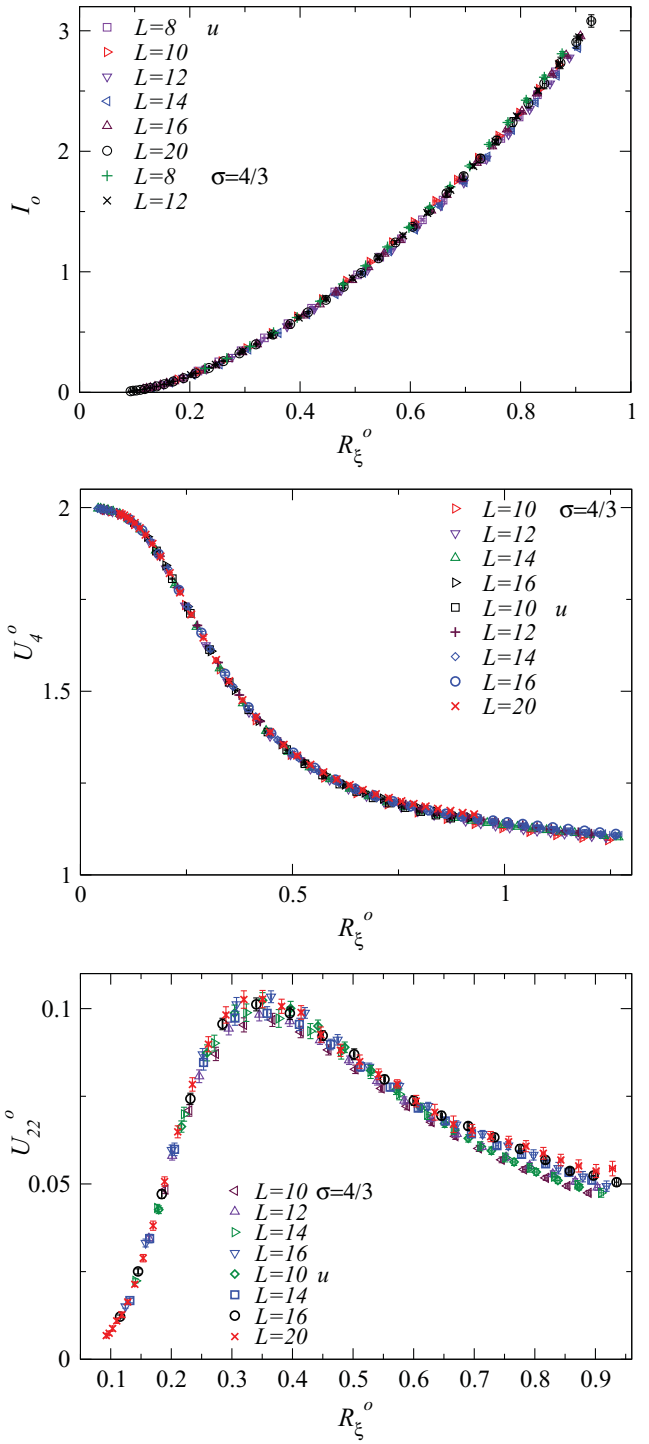

FIG. 4. (Color online) I_o (top), U_4^o (middle) and U_{22}^o (bottom) vs R_ξ^o for $\sigma = 4/3$ and the uniform distribution (denoted by u).

R_ξ is achieved by plotting them versus $(T - T_c)L^{1/\nu_{XY}}$ with $\nu_{XY} = 0.6717$, thus supporting the universality with the pure 3D XY model. Analogous results are obtained for the other RG invariant quantities.

Given two generic RG invariant quantities R_1 and R_2, the relation

$$R_1 = f_{R_1}(R_2) \qquad (14)$$

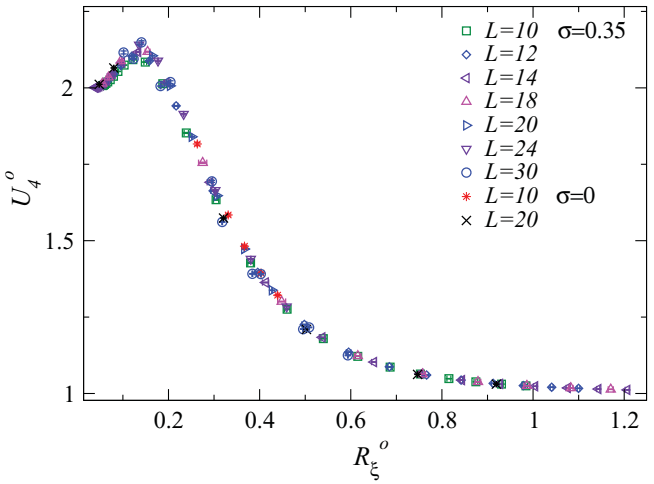

FIG. 5. (Color online) U_4^o vs R_ξ^o at $\sigma = 0.35$ and for the pure XY model ($\sigma = 0$).

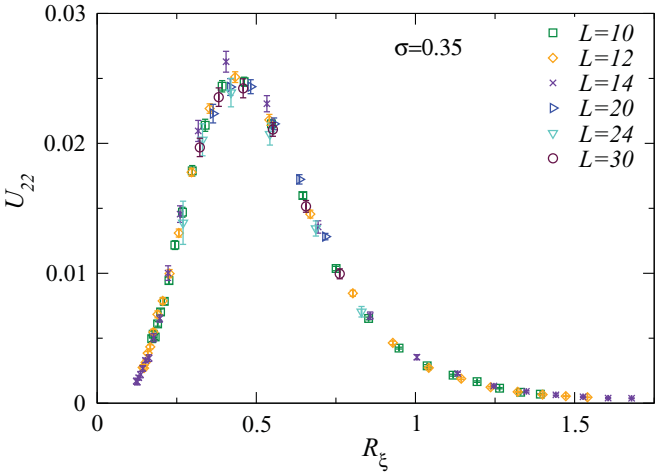

FIG. 6. (Color online) U_{22} vs R_ξ at $\sigma = 0.35$.

is asymptotically universal, i.e., independent of the model within the given universality class, apart from scaling corrections. This fact provides further stringent checks of universality. As an example, Fig. 5 shows a plot of U_4^o versus R_ξ^o from MC simulations of the gauge glass with $\sigma = 0.35$ and of the pure XY model, i.e., $\sigma = 0$. The data appear to approach a unique universal curve in the large-L limit, providing further strong evidence of universality. Analogous results are obtained for other combinations of R_ξ, R_ξ^o, U_4, and U_4^o.

These numerical results provide strong evidence that the critical behavior along the PF transition line belongs to the 3D XY universality class of pure systems. The above-mentioned slowly decaying scaling corrections are best observed in the quantity U_{22}, cf. Eq. (9), which is trivially zero in pure systems. In Fig. 6 we show U_{22} versus R_ξ for several values of L. The data of U_{22} at $\sigma = 0.35$ are very small, $U_{22} < 0.03$, but nonzero. U_{22} is expected to vanish for $L \to \infty$, but very slowly, as

$$U_{22} \sim L^{-\omega_d} \bar{f}_{U_{22}}(R_\xi), \quad \omega_d = 0.0225(5), \tag{15}$$

where $\bar{f}_{22}(R_\xi)$ is a universal function apart from a trivial overall normalization. Without taking into account Eq. (15), the data of U_{22} in Fig. 4 might be considered evidence of an unexpected scaling behavior and, therefore, of a different universality class. However, one can easily check that they are still compatible with a very slow suppression in the large-L limit, such as Eq. (15). Indeed, with increasing the size from $L = 10$ to $L = 30$, the expected variation should be just a few percent, which is within the typical statistical error of the data in Fig. 6. A check of the vanishing large-L limit of U_{22} would require much larger lattices and higher statistics. A similar situation has been met at the PF transition line of the 2D $\pm J$ Ising model, where U_{22} vanishes logarithmically, as shown in Ref. 47.

IV. THE PARAMAGNETIC-GLASSY TRANSITION LINE

In the case of a uniform distribution of random phase shifts, which is formally represented by the limit $\sigma \to \infty$, there is already good numerical evidence, see, e.g., Refs. 25,28, for a finite-T PG transition between the high-T paramagnetic phase and a low-T glassy phase. The glassy phase is expected to persist when we consider finite large values of σ; thus, a PG transition line is expected for sufficiently large values of σ. More precisely, it is expected to run from the large disorder limit down to the multicritical point M, see Fig. 1, at $T_M = \sigma_M \approx 0.784$, see the next section. Our working hypothesis is that the critical behavior along this PG line is universal, belonging to the 3D gauge-glass universality class.

A. Monte Carlo simulations

In order to investigate the glassy critical behavior at large disorder, we present FSS analyses of MC simulations for $\sigma = 4/3$ and for uniformly distributed phase shifts, formally corresponding to $\sigma \to \infty$, up to lattice sizes $L = 16$ and $L = 20$, respectively. We perform averages over 10^4 disorder configurations for all the lattice sizes and temperatures considered.

In these MC simulations we supplement the local MC updating method, used at the PF transition line, with the random-exchange or parallel tempering method, see, e.g., Ref. 48, which allows us to reliably simulate small values of T, in particular, below the N line $T = \sigma$. In the parallel-tempering simulations we consider N_T systems at the same value of σ and at N_T different temperatures in the range $T_{\max} \geqslant T_i \geqslant T_{\min}$, with $T_{\max} \approx 0.87$ and $T_{\min} \approx 0.37$. The value $T_{\max}$ is chosen so that the thermalization at $T_{\max}$ is sufficiently fast, while the intermediate values T_i are chosen so that the acceptance probability of the temperature exchange is at least 5%. Moreover, we require that one of the T_i be along the N line, i.e., $T_i = \sigma$, where the known exact results allow us to check the MC code and the thermalization. The thermalization is further checked by verifying that the averages of the observables remain stable for all T_i after a sufficiently large number of MC steps for each disorder realization. The overlap correlations and the corresponding χ_o and ξ_o are measured by performing two independent runs for each disorder sample. In the case of observables requiring the computation of the disorder average of products of thermal expectations, such as the case of U_{22}^o, we use unbiased estimators as explained in Refs. 4,49 (a naive

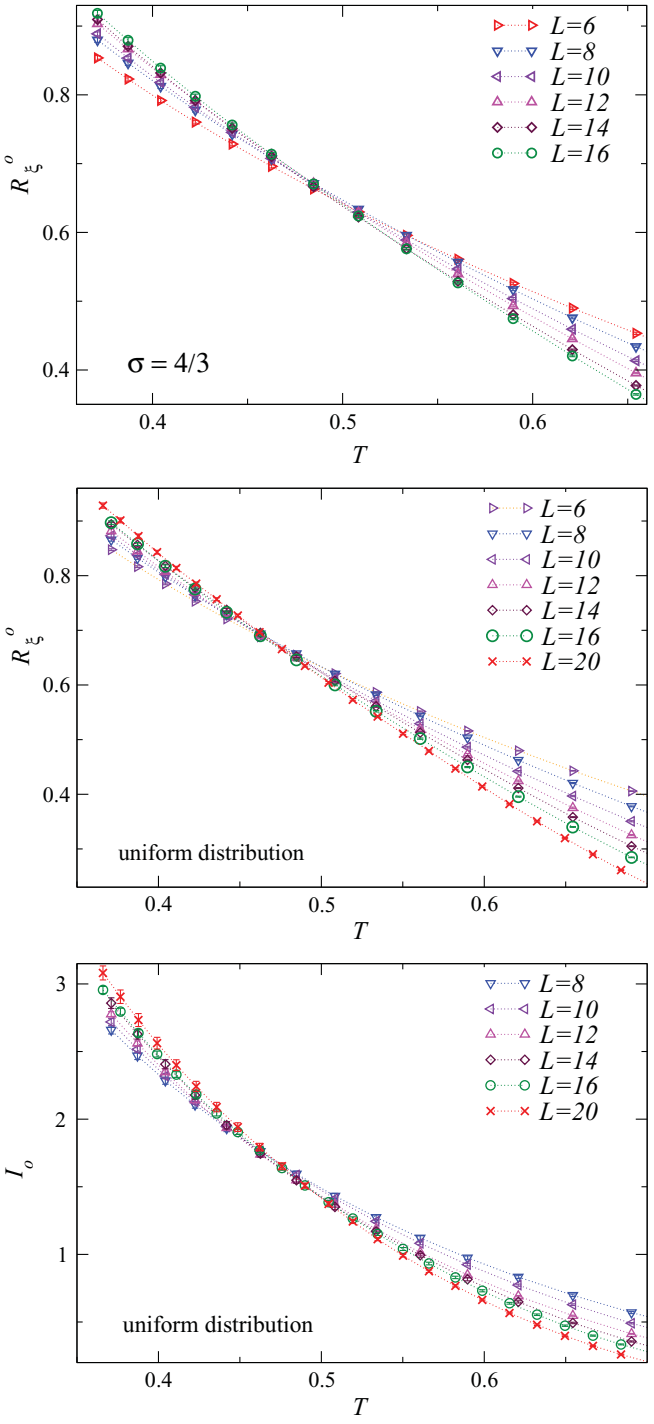

FIG. 7. (Color online) R_ξ^o for $\sigma = 4/3$ (top), and R_ξ^o (middle) and I_o (bottom) for the uniform random-shift distribution.

application of the disorder average would introduce a bias, thus a systematic error).

B. Finite-size scaling analysis

In Fig. 7 we show the MC data of R_ξ^o and I_o, cf. Eq. (11). Their crossing points provide strong evidence of a finite-T transition for both $\sigma = 4/3$ and $\sigma = \infty$. A large exponent ν is already suggested by the slow rising of the slopes at the crossing point with increasing L.

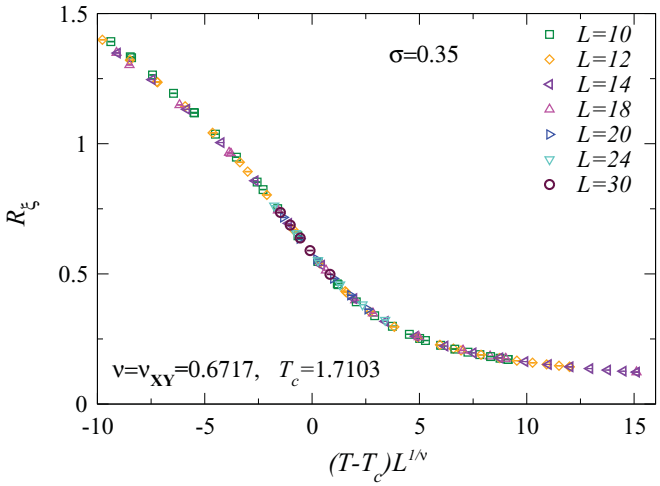

FIG. 8. (Color online) R_ξ vs $(T - T_c)L^{1/\nu_{XY}}$ with $\nu_{XY} = 0.6717$, for $\sigma = 0.35$.

To begin with, we address the universality issue, i.e., whether the transitions at $\sigma = 4/3$ and $\sigma = \infty$ have the same universal critical behavior. For this purpose, in Fig. 8 we plot data of I_o, U_4^o, and U_{22}^o versus R_ξ^o at $\sigma = 4/3$ and $\sigma = \infty$. They appear to converge toward the same universal large-L limit, providing strong evidence of universality. These results support our working hypothesis that the glassy critical behavior is universal along the PG transition line from large disorder to the multicritical point M.

The FSS behavior of the RG invariant quantities allows us to estimate T_c and ν:

$$R(T,L) = f(u_t L^{1/\nu}) = R^* + c_1(T - T_c)L^{1/\nu} + c_2(T - T_c)^2 L^{2/\nu} + \cdots, \quad (16)$$

where R indicates the generic RG invariant quantity, such as R_ξ^o and I_o, u_t is the temperature scaling field, $u_t \sim T - T_c$, and we neglect scaling-correction terms. We check the stability of the fits by increasing the minimum size $L_{\min}$ of the data used in the fit, varying the range of values of T around T_c [we use self-consistent windows around T_c limiting the allowed range of values of $(T - T_c)L^{1/\nu}$, which corresponds to the range of values of any R around R^*], and the number of terms in Eq. (16). We use the comparison of the results using different quantities as a check of the relevance of the neglected scaling corrections. Some results of fits of the data of R_ξ and I_o, using the ansatz (16), are reported in Table I.

In the case of the uniform distribution we have data up to $L = 20$. The fits of the data of R_ξ^o are reasonably stable. We note some oscillations in the estimates of T_c, which may reflect the difficulty of estimating T_c when the critical exponent ν is large. From these results one may get the estimates $T_c = 0.46(1)$, $1/\nu = 0.31(4)$, and $R_\xi^{o*} = 0.70(2)$, where errors take also into account the stability with respect to changes of $L_{\min}$, from $L_{\min} = 6$ to $L_{\min} = 12$, and the range of T around the crossing point. The results using I_o are definitely consistent, although they appear less precise (also because they correspond to less statistics, we started later collecting data for I_o). They suggest the estimates $T_c = 0.47(2)$, $1/\nu = 0.30(5)$, and $I_o^* = 1.7(1)$. The fits of the data for the cumulants U_4^o and

TABLE I. Results of fits to $R^* + \sum_{i=1}^{n} c_i (T - T_c)^i L^{i/\nu}$ of the data of R_ξ^o and I_o, with respect to variations of the range of T (taking data for $|R_\xi^o - R_\xi^{o*}| \leqslant \Delta R_\xi^o$ to have a self-consistent scaling cut, with $R_\xi^{o*} \approx 0.7$), the number n of terms in the fit ansatz, and $L_{\min}$, which is the minimum size allowed by the data.

σ	R	ΔR_ξ	n	$L_{\min}$	T_c	$1/\nu$	R^*	χ^2/dof
∞	R_ξ^o	0.07	1	8	0.467(2)	0.27(3)	0.684(5)	3.1
				10	0.477(3)	0.29(4)	0.665(7)	2.9
				12	0.458(4)	0.31(7)	0.703(9)	1.8
		0.1	1	8	0.465(2)	0.27(2)	0.689(4)	3.6
				10	0.475(2)	0.29(2)	0.669(5)	3.5
				12	0.455(4)	0.29(4)	0.712(9)	2.1
				14	0.461(5)	0.33(6)	0.698(11)	1.8
		0.1	2	8	0.466(2)	0.29(8)	0.687(3)	3.2
		0.2	2	6	0.463(1)	0.31(2)	0.690(2)	3.3
				8	0.460(1)	0.32(2)	0.698(2)	3.0
				10	0.469(2)	0.32(2)	0.680(3)	2.8
				12	0.450(3)	0.29(3)	0.721(6)	1.6
				14	0.456(4)	0.31(4)	0.708(9)	1.3
	I_o	0.1	1	8	0.467(5)	0.26(4)	1.74(5)	1.4
				10	0.472(6)	0.27(5)	1.69(5)	1.5
				12	0.488(7)	0.33(7)	1.53(7)	0.8
		0.3	2	8	0.463(2)	0.38(12)	1.77(2)	1.6
4/3	R_ξ^o	0.1	1	6	0.486(2)	0.31(2)	0.669(4)	2.7
				8	0.477(2)	0.31(2)	0.685(5)	1.5
				10	0.478(5)	0.28(5)	0.683(10)	1.8
		0.1	2	8	0.476(3)	0.31(11)	0.686(4)	1.0
		0.2	2	6	0.479(1)	0.33(2)	0.682(2)	3.1
				8	0.471(2)	0.33(2)	0.695(3)	1.4
				10	0.471(3)	0.31(3)	0.695(6)	1.6

U_{22}^o do not provide sufficiently stable results, but they scale consistently as shown by Fig. 8.

In the case of the distribution with $\sigma = 4/3$, whose data are up to $L = 16$, we obtain $T_c = 0.475(10)$, $1/\nu = 0.32(4)$, and $R_\xi^{o*} = 0.69(1)$ from the fits of the data of R_ξ^o. For $\sigma = 4/3$ we have only few data for I_o, see Fig. 8, which do not allow us to obtain an independent estimate of ν.

The above results for ν are consistent and thus in agreement with universality. We consider

$$1/\nu = 0.31(4), \quad \nu = 3.2(4), \tag{17}$$

our final estimate. Figure 9 shows the collapse of the data of R_ξ^o and I_o for the gauge glass with uniform distribution, when they are plotted versus $(T - T_c)L^{1/\nu}$, with $T_c = 0.46$ and $1/\nu = 0.31$. Note that ν is quite large but still comparable to the value $\nu = 2.45(15)$ of the glassy transition in 3D Ising-like spin glasses.[4,40,41] We should also say that the accuracy and the relatively small lattice size of the available data do not allow us a robust control of the neglected scaling-corrections, as was achieved for the Ising-like spin glass models.[50] Therefore, further numerical work is required to substantiate the above results.

We compute the exponent η associated with the overlap correlation (4) by analyzing the data of the overlap susceptibility χ_o, which is expected to behave as[4]

$$\chi_o = \overline{u}_h^2 L^{2-\eta_o} f(u_t L^{1/\nu}). \tag{18}$$

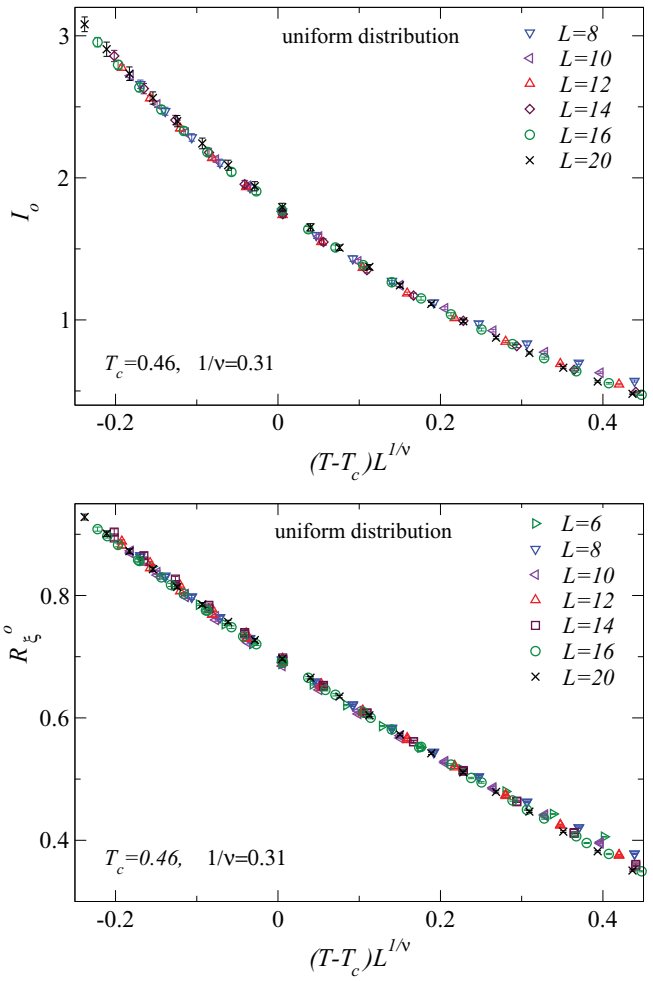

FIG. 9. (Color online) I_o (top) and R_ξ^o (bottom) vs $(T - T_c)L^{1/\nu}$ for the uniform distribution, with $T_c = 0.46$ and $1/\nu = 0.31$.

Here $\overline{u}_h$ is related to the external overlap scaling field u_h associated with the overlap variables by $u_h = h\overline{u}_h(T) + O(h^2)$. Thus, neglecting nonanalytic scaling corrections, we fit the data of χ_o to

$$\ln \chi_o = a \ln L + b_0 + b_1(T - T_c) + \cdots + c_1(T - T_c)L^{1/\nu} + \cdots, \tag{19}$$

fixing the values of T_c and ν as obtained above. We obtain

$$\eta = -0.47(2) \tag{20}$$

for the uniform distribution and $\eta = -0.46(2)$ for the distribution with $\sigma = 4/3$, where the error takes also into account the uncertainty on T_c and ν.

Finally, we compare our results with earlier numerical works for the gauge-glass model with uniformly distributed random phase shifts. Earlier estimates of T_c, i.e., $T_c = 0.47(3)$ from Ref. 25 and $T_c = 0.48(2)$ from Ref. 30, are consistent with ours. Our result $\nu = 3.2(4)$ is significantly larger than the estimates obtained by earlier FSS analyses, $\nu = 1.3(4)$ from Ref. 19, $\nu = 1.39(20)$ from Ref. 25, and $\nu = 1.62(20)$ Ref. 30. These smaller values of ν appear excluded by our FSS analyses. This discrepancy may be explained by the

small lattice sizes, up to $L = 12$, of their data. We also mention that our estimate is larger than the experimental estimate at the vortex-glass transition in the (K,Ba)BiO_3 cubic superconductor reported in Ref. 33, i.e., $\nu = 1.0(2)$, which has been often compared with the glassy transition of the gauge glass with uniform distribution. Finally, our estimate (20) of η agrees with the result $\eta = -0.47(7)$ reported in Ref. 25.

V. THE MULTICRITICAL POINT ALONG THE N LINE

In the case of the cosine distribution (2), the N line plays an important role in the phase diagram, because it marks the crossover between the magnetic-dominated region and the disorder-dominated one. We conjecture that the PF and PG transition lines meet at a multicritical point M, which coincides with the critical point along the N line, analogously to the phase diagram of the 3D $\pm J$ Ising model.[4,17,43] It is worth mentioning that the critical point along the N line shows a multicritical behavior also in the 2D $\pm J$ Ising model and 2D gauge glass, see, e.g., Refs. 14,51,52, even though these models do not have a low-T glassy phase.

We shall support the above scenario by a FSS of MC simulations of the 3D gauge glass along the N line.

A. The Nishimori line

The cosine distribution (2) lends itself to some exact calculations along the N line.[16,17] For example, the energy density is[16] $E = -3I_1(1/T)/I_0(1/T)$ when $T = \sigma$, where I_i are modified Bessel functions. Moreover, the spin and overlap correlation functions are equal:

$$[\langle \bar{\psi}_x \psi_y \rangle] = [|\langle \bar{\psi}_x \psi_y \rangle|^2]. \tag{21}$$

Along the N line we also have $R_\xi = R_\xi^o$ and $U_4 = U_4^o$.

As proved in Ref. 16, the critical value σ_M of σ along the N line is an upper bound for the values of σ where the ferromagnetic long-range order can exist. Therefore, at the critical point $M \equiv (\sigma_M, T_M)$ the tangent to the transition line limiting the ferromagnetic phase must be parallel to the T axis; moreover, the critical value σ_D where the ferromagnetism disappears at $T = 0$ must satisfy $\sigma_D \leqslant \sigma_M$.

The N line $T = \sigma$ is also characterized by an extension of the replica symmetry. The quenched average over disorder, which implies the average of the free energy, can be formally reconstructed by introducing n replicas of the system, taking the limit $n \to 0$ after the disorder average. We write the disorder average over the partition function of n replicas as

$$[Z^{(n)}(A)] = \int [DA] \exp\left[(1/\sigma)\sum_{\langle xy\rangle} \cos A_{xy}\right] \int \prod_n [D\psi^{(n)}] \times \exp\left[(1/T)\sum_{\langle xy\rangle} \cos\left(\theta_x^{(n)} - \theta_y^{(n)} - A_{xy}\right)\right]. \tag{22}$$

Let us perform the gauge transformation

$$\psi_x \to e^{i\varphi_x}\psi_x, \quad U_{xy} \to e^{-i\varphi_x} U_{xy} e^{i\varphi_y}. \tag{23}$$

We obtain

$$[Z^{(n)}(A)] = \int [DA] \exp\left[(1/\sigma)\sum_{\langle xy\rangle} \cos(\varphi_x - \varphi_y - A_{xy})\right] \times \int \prod_n [D\psi^{(n)}] \exp\left[(1/T)\sum_{\langle xy\rangle} \cos\left(\theta_x^{(n)} - \theta_y^{(n)} - A_{xy}\right)\right]. \tag{24}$$

Since a further integration with respect to $\phi_x \equiv e^{i\varphi_x}$ gives rise only to a trivial constant factor, we have that the gauge variables ϕ_x correspond to another identical replica when $T = \sigma$, extending the original replica symmetry.

B. Scaling behavior at the multicritical point

As a working hypothesis, we assume that the critical point along the N line is a multicritical point, analogously to the case of the 3D $\pm J$ Ising model.[43] We derive some predictions which are then verified by a FSS analysis of numerical MC simulations.

In the absence of external fields, the critical behavior at the multicritical point M is characterized by two relevant RG operators. The singular part of the free energy averaged over disorder in a volume of size L can be written as

$$F_{\rm sing}(T,\sigma,L) = L^{-d} f(u_1 L^{y_1}, u_2 L^{y_2}, \{u_i L^{y_i}\}), \tag{25}$$

with $i \geqslant 3$, where $y_1 > y_2 > 0$, $y_i < 0$ for $i \geqslant 3$, u_i are the corresponding scaling fields, and $u_1 = u_2 = 0$ at M. In the infinite-volume limit and neglecting subleading corrections, we have

$$F_{\rm sing}(T,\sigma) = |u_2|^{d/y_2} f_\pm(u_1 |u_2|^{-\phi}) \tag{26}$$

around M, with $\phi = y_1/y_2 > 1$, where the functions $f_\pm(x)$ apply to the parameter regions in which $\pm u_2 > 0$. Close to M, all transition lines correspond to constant values of the product $u_1|u_2|^{-\phi}$ and thus, since $\phi > 1$, they are tangent to the line $u_1 = 0$.

The relevant scaling fields u_1 and u_2 can be inferred by using the following facts: (i) Since σ_M is an upper bound for the values of σ where the ferromagnetic phase can exist, the transition line at M must be parallel to the T axis; (ii) the condition $T = \sigma$ at the N line is RG invariant, because it is protected by the extension of the replica symmetry, as shown in Sec. V A. We therefore have

$$u_1 = \sigma - \sigma_M + \cdots, \tag{27}$$

where the dots indicate nonlinear corrections, which are quadratic in $\Delta\sigma \equiv \sigma - \sigma_M$ and $\Delta T \equiv T - T_M$, so that the line $u_1 = 0$ runs parallel to the T axis at M. Moreover, we choose

$$u_2 = T - \sigma, \tag{28}$$

so that the N line corresponds to $u_2 = 0$.

These results give rise to the following predictions for the FSS behavior around M. Let us consider a RG invariant quantity R, such as R_ξ, U_4, U_{22}, defined in Sec. II. In general, in the FSS limit R obeys the scaling law

$$R = \mathcal{R}(u_1 L^{y_1}, u_2 L^{y_2}, \{u_i L^{y_i}\}), \quad i \geqslant 3. \tag{29}$$

Neglecting the scaling corrections which vanish in the limit $L \to \infty$, we expect

$$R = R^* + b_{11} u_1 L^{y_1} + b_{21} u_2 L^{y_2} + \cdots . \quad (30)$$

Along the N line, the scaling field u_2 vanishes, so that we can write

$$R_N = R^* + b_{11} u_1 L^{y_1} + b_{12} u_1^2 L^{2y_1} + \cdots , \quad (31)$$

where the subscript N indicates that R is restricted to the N line. Differentiating Eq. (30) with respect to $\beta \equiv 1/T$, we obtain

$$R' = b_{11} u_1' L^{y_1} + b_{21} u_2' L^{y_2} + \cdots . \quad (32)$$

If Eq. (27) holds, then $u_1' = O(T - T_M)$, so that the leading behavior along the N line is

$$R_N' = b_{21} u_2' L^{y_2} + \cdots . \quad (33)$$

The magnetic susceptibility along the N line behaves as

$$\chi_N = e L^{2-\eta} (1 + e_1 u_1 L^{y_1} + \cdots). \quad (34)$$

Note that there is only one η exponent which characterizes the critical behavior of both the magnetic and overlap correlation functions, since they are equal along the N line.

C. MC results

In the following we present a FSS analysis of MC simulations along the N line. The MC algorithm was a mixture of standard Metropolis and overrelaxed microcanonical updates, as in the MC simulations at the PF transition line reported in Sec. III. In order to locate the multicritical point we simulated several temperatures ranging from $T = 0.773$ to $T = 0.797$, for lattice sizes $6 \leqslant L \leqslant 20$. The number of disorder configurations ranged from 4×10^5 to 2×10^7 for the largest lattices. This large statistics was necessary to achieve a convincing evidence of the multicritical nature of M.

The MC data of R_ξ are shown in Fig. 10. There is clearly a crossing point at $T \approx 0.784$. Analogous results are obtained from U_4 and U_{22}. In order to estimate T_M and y_1, we fit the

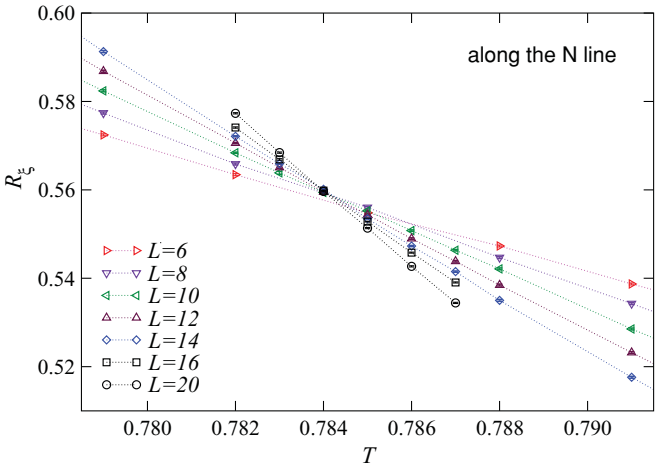

FIG. 10. (Color online) R_ξ along the N line $T = \sigma$.

RG invariant R to

$$R = R^* + a_1 (T - T_M) L^{y_1} + a_2 (T - T_M)^2 L^{2y_1} + \cdots . \quad (35)$$

Note that this functional form relies on the property that $u_2 = 0$ along the N line. Otherwise, an additional term of the form $(T - T_M) L^{y_2}$ should be added. We also neglect scaling corrections which are $O(L^{y_3})$ with $y_3 < 0$. We check their relevance by comparing results from the analyses of different quantities.

Our best estimates are

$$T_M = \sigma_M = 0.7840(2), \quad (36)$$

$$y_1 = 0.93(3), \quad (37)$$

and also $R_\xi^* = 0.5594(4)$, $U_4^* = 1.226(1)$, and $U_{22}^* = 0.128(4)$. The errors take into account the stability of the results with respect to the minimum size $L_{\min}$ allowed in the fits (typically from $L_{\min} = 6$ to $L_{\min} = 12$), the range of values of T around T_c [we use again self-consistent windows around T_c limiting the allowed range of values of $(T - T_M) L^{y_1}$], and the number of terms in Eq. (35). Scaling corrections are apparently small. We find some evidence of scaling corrections only in the analysis of U_{22}, but they appear to decay quite fast, suggesting a relatively large scaling correction exponent, i.e., $y_3 \approx -2$.

The derivative R' with respect to β can be estimated by computing appropriate connected correlations of R and the Hamiltonian in the MC simulations along the N line. According to the multicritical scenario outlined above, R' is expected to behave as L^{y_2} at T_M with $y_2 < y_1$. In order to determine y_2, we fit the data to

$$\ln R' = a + y_2 \ln L + b(T - T_M) L^{y_1}, \quad (38)$$

keeping $T_M = 0.7840$ and $y_1 = 0.93$ fixed. We obtain

$$y_2 = 0.56(3) \quad (39)$$

from R_ξ' (the error includes the uncertainty on T_M and y_1). The data of U_4' are not sufficiently precise to provide a stable result. The above estimate of y_2 nicely supports the multicritical scenario, since it shows that $y_2 < y_1$. Therefore the crossover exponent, cf. Eq. (26), is

$$\phi = \frac{y_1}{y_2} = 1.7(1). \quad (40)$$

We determine the exponent η from the FSS of the ratio $Z \equiv \chi/\xi^2 \sim L^{-\eta}$ at the critical point. We fit its MC data along the N line to

$$\ln Z = a - \eta \ln L + b(T - T_M) L^{y_1} + c(T - T_M), \quad (41)$$

where the last term takes into account possible analytic terms coming from the scaling fields,[4] analogously to Eq. (18). We obtain

$$\eta = -0.121(1). \quad (42)$$

It is worth noting that the above estimates of the multicritical exponents are quite close to those found for the 3D $\pm J$ Ising model, at the multicritical point along its N line, where[43] $y_1 = 1.02(5)$, $y_2 = 0.61(2)$, $\phi = 1.67(10)$, and $\eta = -0.114(3)$.

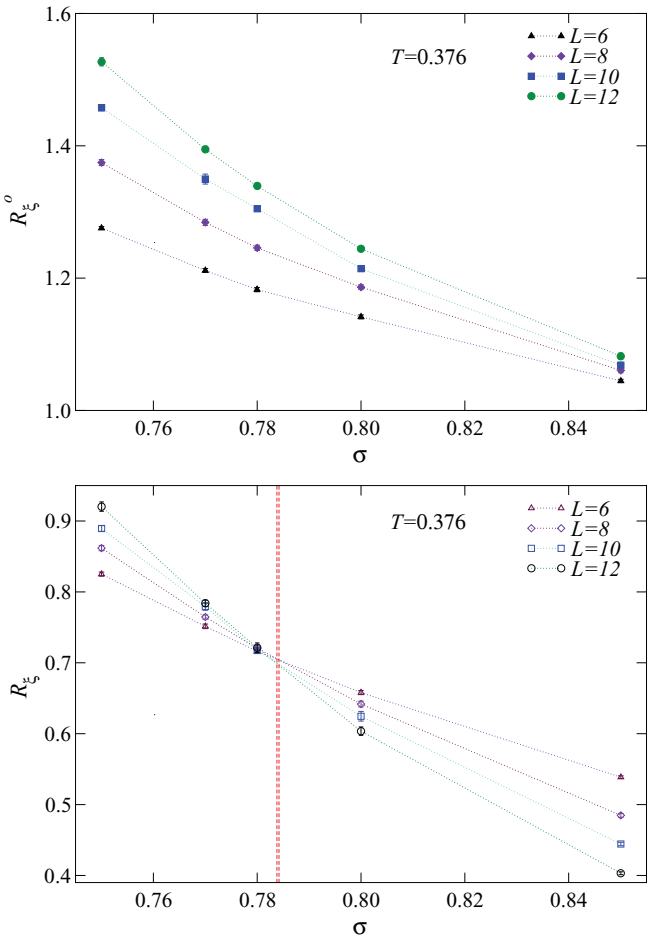

FIG. 11. (Color online) R_ξ (bottom) and R_ξ^o (top) at $T = 0.376$ across the FG transition line. The vertical dashed lines show the estimate of σ_M, i.e., $\sigma_M = 0.7840(2)$, with its uncertainty.

VI. THE FERROMAGNETIC-GLASSY TRANSITION LINE

The FG transition line runs from the multicritical point down to $T = 0$, with $\sigma_c \leqslant \sigma_M$, since σ_M provides a bound for the region where the magnetic order can exist. The order parameter along this transition is provided by the magnetic variables and their correlations.

Reference 16 argues that this transition line runs parallel to the T axis, thus $\sigma_c = \sigma_M$ for $T < T_M$. An analogous prediction for the 2D $\pm J$ Ising model turns out to fail, although it provides a good approximation, because the low-T transition line where ferromagnetism disappears turns out to be slightly reentrant, see, e.g., Refs. 52,53 and references therein.

We investigate this issue by numerical MC simulations up to lattice sizes $L = 12$, using the same MC method employed at the glassy transitions. Using random-exchange MC simulations, we collect data down to $T = 0.376$ for several values of σ in the range $0.75 \leqslant \sigma \leqslant 0.85$. Our results are obtained by averaging over a large number of of disorder configurations: $N_s = 16000, 8000, 6000, 4000$ respectively for $L = 6, 8, 10, 12$. Figure 11 shows the data of R_ξ and R_ξ^o at $T = 0.376$. The set of data of R_ξ for different lattice sizes show a crossing point, confirming the existence of FG transition. On the contrary, the data of R_ξ^o do not show crossings, which may reflect the fact that such transition separates two *ordered* phases with respect to the overlap variables.

The crossing points of the R_ξ data appear to cluster at a value of σ which is slightly smaller than $\sigma_M = 0.7840(2)$. Indeed, fitting them to

$$R_\xi = R_\xi^* + a_1(\sigma - \sigma_c)L^{1/\nu} + a_2(\sigma - \sigma_c)^2 L^{2/\nu} + \cdots, \quad (43)$$

we obtain

$$\sigma_c = 0.777(2), \quad \nu = 1.0(1), \quad (44)$$

and $R_\xi^* = 0.73(1)$. These estimates should be taken with some caution, in particular that of ν, due to the small size of the available lattices, which does not allow us to perform stringent checks of stability. The analysis of the data of U_4 gives consistent results, but less precise. We also mention that an analogous FSS analysis of the data at a larger temperature $T = 0.437$, but still smaller than T_M, gives $\sigma_c = 0.782(2)$, $\nu = 1.1(1)$, and $R_\xi^* = 0.71(1)$, which supports the universality of the magnetic critical behavior along the FG transition line.

According to the above results, the critical values of the disorder parameter at $T < T_M$ are very close to but smaller than $\sigma_M = 0.7840(2)$, indicating a slight reentrant transition line.

ACKNOWLEDGMENTS

The MC simulations were performed at the INFN Pisa GRID DATA center, using also the cluster CSN4. In total, they took approximately 100 years of CPU time on a single core of a recent standard commercial processor.

*vincenzo@pks.mpg.de
†ettore.vicari@df.unipi.it

[1] S. F. Edwards and P. W. Anderson, J. Phys. F **5**, 965 (1975).
[2] A. P. Young, ed., *Spin Glasses and Random Fields* (World Scientific, Singapore, 2004).
[3] N. Kawashima and H. Rieger, in *Frustrated Spin Systems*, edited by H. T. Diep (World Scientific, Singapore, 2004).
[4] M. Hasenbusch, A. Pelissetto, and E. Vicari, Phys. Rev. B **78**, 214205 (2008).
[5] L. A. Fernandez, V. Martin-Mayor, S. Perez-Gaviro, A. Tarancon, and A. P. Young, Phys. Rev. B **80**, 024422 (2009).
[6] D. X. Viet and H. Kawamura, Phys. Rev. B **80**, 064418 (2009).
[7] W. Y. Shih, C. Ebner, and D. Stroud, Phys. Rev. B **30**, 134 (1984).
[8] E. Granato and J. M. Kosterlitz, Phys. Rev. B **33**, 6533 (1986); Phys. Rev. Lett. **62**, 823 (1989).
[9] S. John and T. C. Lubensky, Phys. Rev. B **34**, 4815 (1986).
[10] D. A. Huse and H. S. Seung, Phys. Rev. B **42**, 1059 (1990).
[11] M. P. A. Fisher, T. A. Tokuyasu, and A. P. Young, Phys. Rev. Lett. **66**, 2931 (1991).
[12] G. Blatter, M. V. Feigelman, V. B. Geshkenbein, A. I. Larkin, and V. M. Vinokur, Rev. Mod. Phys. **66**, 1125 (1994).
[13] T. Nattermann and S. Scheidl, Adv. Phys. **49**, 1465 (2000).
[14] V. Alba, A. Pelissetto, and E. Vicari, J. Stat. Mech. Theory Exp. (2010) P03006.

[15]S. E. Korshunov, Usp. Fiz. Nauk **176**, 233 (2006) [Phys. Usp. **49**, 225 (2006)].
[16]Y. Ozeki and H. Nishimori, J. Phys. A **26**, 3399 (1993).
[17]H. Nishimori, *Statistical Physics of Spin Glasses and Information Processing: An Introduction* (Oxford University Press, Oxford, 2001).
[18]M. S. Li, T. Nattermann, H. Rieger, and M. Schwartz, Phys. Rev. B **54**, 16024 (1996).
[19]J. D. Reger, T. A. Tokuyasu, A. P. Young, and M. P. A. Fisher, Phys. Rev. B **44**, 7147 (1991).
[20]M. J. P. Gingras, Phys. Rev. B **44**, 7139 (1991); **45**, 7547 (1992).
[21]M. Cieplak, J. R. Banavar, and A. Khurana, J. Phys. A **24**, L145 (1991).
[22]J. M. Kosterlitz and M. V. Simkin, Phys. Rev. Lett. **79**, 1098 (1997).
[23]C. Wengel and A. P. Young, Phys. Rev. B **56**, 5918 (1997).
[24]J. Maucourt and D. R. Grempel, Phys. Rev. B **58**, 2654 (1998).
[25]T. Olson and A. P. Young, Phys. Rev. B **61**, 12467 (2000).
[26]H. G. Katzgraber and A. P. Young, Phys. Rev. B **64**, 104426 (2001).
[27]N. Akino and J. M. Kosterlitz, Phys. Rev. B **66**, 054536 (2002).
[28]H. G. Katzgraber and A. P. Young, Phys. Rev. B **66**, 224507 (2002).
[29]H. G. Katzgraber and I. A. Campbell, Phys. Rev. B **72**, 014462 (2005).
[30]H. G. Katzgraber, D. Würtz, and G. Blatter, Phys. Rev. B **75**, 214511 (2007).
[31]F. Romá and D. Domínguez, Phys. Rev. B **78**, 184431 (2008).
[32]R. H. Koch, V. Foglietti, W. J. Gallagher, G. Koren, A. Gupta, and M. P. A. Fisher, Phys. Rev. Lett. **63**, 1511 (1989).
[33]T. Klein, A. Conde Gallardo, J. Marcus, C. Escribe-Filippini, P. Samuely, P. Szabó, and A. G. M. Jansen, Phys. Rev. B **58**, 12411 (1998).
[34]A. M. Petrean, L. M. Paulius, W.-K. Kwok, J. A. Fendrich, and G. W. Crabtree, Phys. Rev. Lett. **84**, 5852 (2000).
[35]D. R. Strachan, M. C. Sullivan, P. Fournier, S. P. Pai, T. Venkatesan, and C. J. Lobb, Phys. Rev. Lett. **87**, 067007 (2001).
[36]I. L. Landau and H. R. Ott, Phys. Rev. B **65**, 064511 (2002).
[37]M. Campostrini, M. Hasenbusch, A. Pelissetto, and E. Vicari, Phys. Rev. B **74**, 144506 (2006).
[38]A. Pelissetto and E. Vicari, Phys. Rep. **368**, 549 (2002).
[39]M. Hasenbusch, F. Parisen Toldin, A. Pelissetto, and E. Vicari, Phys. Rev. B **76**, 094402 (2007).
[40]H. G. Katzgraber, M. Körner, and A. P. Young, Phys. Rev. B **73**, 224432 (2006).
[41]H. G. Ballesteros, A. Cruz, L. A. Fernández, V. Martín-Mayor, J. Pech, J. J. Ruiz-Lorenzo, A. Tarancón, P. Téllez, C. L. Ullod, and C. Ungil, Phys. Rev. B **62**, 14237 (2000).
[42]M. Palassini and S. Caracciolo, Phys. Rev. Lett. **82**, 5128 (1999).
[43]M. Hasenbusch, F. Parisen Toldin, A. Pelissetto, and E. Vicari, Phys. Rev. B **76**, 184202 (2007).
[44]V. Alba, A. Pelissetto, and E. Vicari, J. Phys. A **42**, 295001 (2009).
[45]A. Aharony, in *Phase Transitions and Critical Phenomena*, Vol. 6, edited by C. Domb and M. S. Green (Academic Press, New York, 1976), p. 357.
[46]A. B. Harris, J. Phys. C **7**, 1671 (1974).
[47]M. Hasenbusch, F. Parisen Toldin, A. Pelissetto, and E. Vicari, Phys. Rev. E **78**, 011110 (2008).
[48]D. J. Earl and M. W. Deem, Phys. Chem. Chem. Phys. **7** 3910 (2005).
[49]M. Hasenbusch, F. Parisen Toldin, A. Pelissetto, and E. Vicari, J. Stat. Mech. Theory Exp. (2007) P02016.
[50]M. Hasenbusch, A. Pelissetto, and E. Vicari, J. Stat. Mech. Theory Exp. (2008) L02001.
[51]M. Hasenbusch, F. Parisen Toldin, A. Pelissetto, and E. Vicari, Phys. Rev. E **77**, 051115 (2008).
[52]M. Picco, A. Honecker, and P. Pujol, J. Stat. Mech. Theory Exp. (2006) P09006.
[53]F. Parisen Toldin, A. Pelissetto, and E. Vicari, J. Stat. Phys. **135**, 1039 (2009); Phys. Rev. E **82**, 021106 (2010).